ACS APPLIED MATERIALS & INTERFACES

Research Article

www.acsami.org

Anisotropic Assembly of Conjugated Polymer Nanocrystallites for Enhanced Charge Transport

Mincheol Chang,[†] Jiho Lee,[†] Ping-Hsun Chu,[†] Dalsu Choi,[†] Byoungnam Park,[∥] and Elsa Reichmanis*[,†,‡,§]

[†]School of Chemical and Biomolecular Engineering, [‡]School of Chemistry and Biochemistry, and [§]School of Materials Science and Engineering, Georgia Institute of Technology, Atlanta, Georgia 30332-0100, United States

[∥]Department of Materials Science and Engineering, Hongik University, Seoul 121-791, Korea

Supporting Information

ABSTRACT: The anisotropic assembly of P3HT nanocrystallites into longer nanofibrillar structures was demonstrated via sequential UV irradiation after ultrasonication to the pristine polymer solutions. The morphology of resultant films was studied by atomic force microscopy (AFM), and quantitative analysis of intra- and intermolecular ordering of polymer chains was performed by means of static absorption spectroscopy and quantitative modeling. Consequently, the approach to treat the precursor solution enhanced intra- and intermolecular ordering and reduced the incidence of grain boundaries within P3HT films, which contributed to the excellent charge carrier transport characteristics of the corresponding films ($\mu \approx 12.0 \times 10^{-2}$ cm^2 V^{-1} s^{-1} for 96% RR P3HT).

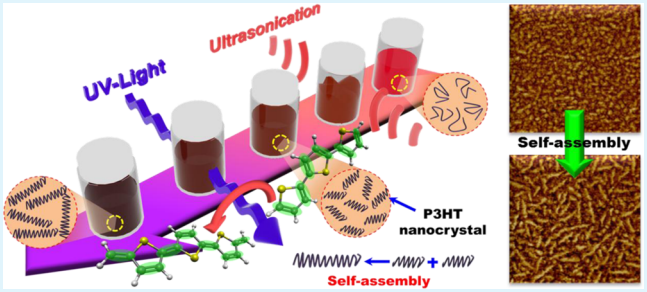

KEYWORDS: *anisotropic assembly, poly(3-hexylthiophene), nanofibers, organic field effect transistors, molecular ordering*

INTRODUCTION

Conjugated polymer (CP) semiconductors are promising materials for a variety applications including light-emitting diodes,[1−3] optical and amperometric sensors,[4−7] organic solar cells,[8−10] and thin-film transistors,[11−14] because of their low-temperature, solution-based processability, which may provide for low-cost, large-area electronic device fabrication.[9,11,14−16] However, CP thin-film charge carrier transport is still relatively lower than that observed for their small molecule organic semiconductor counterparts. CPs generally exhibit lower molecular ordering in solidified thin-films;[17,18] solution processed polymers are semicrystalline, comprised of many small crystalline regions embedded within a largely disordered matrix impeding efficient charge hopping between transport sites.[15,16,19]

Regioregular poly(3-hexylthiophene) (P3HT) is a representative polymer semiconductor investigated for use in a variety of polymer-based organic devices; P3HT self-organizes into a microcrystalline structure,[16,20−22] exhibits acceptable hole transport properties,[23] and exhibits good solubility in selected organic solvents.[15,24] Self-assembled P3HT aggregates exhibit dramatically improved crystallinity and macroscopic charge transport characteristics compared to comparatively more amorphous films, because of enhanced intra- and intermolecular ordering of the polymer chains.[12,16,25] Polymer chain molecular ordering can be influenced by a range of processing techniques such as polymer−dielectric interface treatments,[26] film deposition methods (spin-coating, dip-coating, and drop-casting),[20,27] the use of high-boiling-point solvents,[28] and postdeposition processing (solvent vapor and thermal annealing),[29,30] as well as improved molecular design (regioregularity (RR) and molecular weight (MW)).[20,31,32] However, such strategies present limitations for large-scale fabrication and high-throughput processing because of associated additional treatments before and/or after polymer film deposition.

To eliminate the additional pre- and/or postdeposition steps, several approaches such as tuning solubility,[15,24] solution aging,[33] and ultrasonic irradiation[16] have been explored to induce formation of well-ordered nanofibrillar aggregates in solution, prior to thin-film deposition. In particular, ultrasonic irradiation readily generates crystalline nanofibrillar P3HT aggregates from solutions of the polymer.[16,27] The aggregates survive a spin-coating process, and in turn impart the corresponding polymer films with a higher degree of intra- and intermolecular ordering, resulting in significant enhancement in charge carrier mobility (e.g., from ∼1.6×10^{-2} up to 7.3×10^{-2} cm^2 V^{-1} s^{-1} for 96% RR P3HT).[25] Alternative approaches requiring steps such as the addition of small quantities of poor solvent to the majority solution, and/or aging the solutions to obtain well-ordered aggregates, also afford a mobility enhancement, but to a lesser extent.[15,24,33] However, because of strong agitation associated with the method, ultrasonication restricts nanofibrillar structure growth to less than approximately 200 nm in length,[16,25] and thus grain boundaries between aggregates which will invariably be present in resultant thin films will limit charge transport.

Received: September 23, 2014
Accepted: October 27, 2014
Published: October 27, 2014

Recently, it was demonstrated that low intensity, limited duration ultraviolet (UV) irradiation is an alternative strategy to enhance anisotropic supramolecular ordering of CP chains in solution.[25] Exposure of P3HT solutions to a low UV dose led to highly ordered P3HT aggregates in solution, which was attributed to a conformational change of the polymer chains from "aromatic-" to "quinoid-like" upon photoexcitation.[25] The aggregates were nanofibrillar in appearance, where the fibers were longer than 1 μm in length. The extended structures presumably decreased the number of grain boundaries within the films, resulting in dramatic enhancement of charge carrier mobility up to ~8.2 × 10^{-2} cm^2 V^{-1} s^{-1} for 96% RR P3HT.[25]

Ultrasonication of P3HT precursor solutions is an effective way to increase the crystallinity of resultant films, while low-intensity UV irradiation tends to afford films possessing longer-range ordered aggregates.[25] Such methods were found to cause no discernible change of P3HT MW for 8 min of irradiation owing to mild exposure dose.[16,25] Both molecular ordering of the polymer chains and grain boundaries between the polymer crystallites are key factors impacting CP thin-film charge transport characteristics; enhanced molecular ordering between polymer chains is desirable, while the formation of grain boundaries must be suppressed to maximize transport.

Herein, we demonstrate that sequential ultrasonication and UV irradiation of P3HT solutions, compared to treatment via either method alone, very significantly further improves charge transport characteristics of the resultant films. P3HT nanocrystallites formed upon ultrasonication were anisotropically self-assembled into longer nanofibrillar structures by subsequent UV irradiation of the sonicated solutions. Consequently, the hole transport performance, as determined by mobility of the resultant thin-films, was dramatically enhanced up to ~12.0 × 10^{-2} cm^2 V^{-1} s^{-1} for 96% RR P3HT (P3HT1), a value that is higher than any previously reported for P3HT OFETs prepared without additional steps. The approach also effected an order of magnitude improvement in mobility for 92% RR P3HT (P3HT2) (~0.4 × 10^{-2} for untreated samples, up to 4.4 × 10^{-2} cm^2 V^{-1} s^{-1} for solutions undergoing the sequential treatment). Studies on morphology and intra- and intermolecular ordering of P3HT thin-films reveal that the excellent charge carrier transport demonstrated by OFET measurements is attributable to both a reduction in the number of grain boundaries and enhanced molecular ordering of the polymer thin-films.

RESULTS AND DISCUSSION

Two P3HT polymers (referred to as P3HT1 and P3HT2) were evaluated as representative CPs (Table 1); P3HT1 has 96% RR and 43.7 kDa MW, whereas P3HT2 has 92% RR and 69.0 kDa MW. Figure 1 represents the field effect mobility for P3HT1 and P3HT2 films spin-coated from solutions treated by sequential ultrasonication and UV irradiation for times ranging from 0 to 6 min, respectively. Consistent with earlier reports, P3HT mobility increased (from 2.3 × 10^{-2} to 8.5 × 10^{-2} cm^2 V^{-1} s^{-1} for P3HT1 and from 0.4 × 10^{-2} to 2.0 × 10^{-2} cm^2 V^{-1} s^{-1} for P3HT2) after ultrasonication for 2 min, followed by a mobility decrease with further ultrasonication, presumably owing to an increase in the number of grain boundaries (see AFM images, 2 min sonicated P3HT1 in Figure 2b and 6 min sonicated P3HT1 in Figure 2c) and decreased film thickness (see Figure S1 in the Supporting Information). Meanwhile, mobility increased and then gradually saturated (up to 9.1 × 10^{-2} cm^2 V^{-1} s^{-1} for P3HT1 and 2.0 × 10^{-2} cm^2 V^{-1} s^{-1} for P3HT2) with increased UV irradiation time. Significantly, UV irradiation of P3HT solutions that had undergone ultrasonication led to further enhancements in mobility. Upon ultrasonication and/or UV irradiation times, average mobility with standard error for both P3HT1 and P3HT2 is tabulated in the Supporting Information (Table S1). In particular, the mobility of P3HT1 OFET devices reached a maximum value of 12.0 × 10^{-2} cm^2 V^{-1} s^{-1} when precursor solutions were sequentially treated with 2 min ultrasonication followed by 6 min UV irradiation (Figure 1a). This value is the highest recorded for P3HT devices, fabricated without use of additional steps such as dielectric surface modification and/or thermal or solvent vapor annealing, and is comparable to devices obtained using these methods.[14,28,30,34] P3HT2 device performance was also enhanced up to 4.4 × 10^{-2} cm^2 V^{-1} s^{-1} through 2 min ultrasonication followed by 4 min UV irradiation of the corresponding P3HT precursor solutions (Figure 1b). Figure 1c and d depict P3HT1 transfer and characteristic output curves, respectively, which are typical of p-channel OFET operation in the accumulation mode. The high turn-on voltages (V_{ON}) obtained in Figure 1c are attributed to the effects of residual doping, acceptor like traps at the P3HT-oxide interface, and/or charge trapping at grain boundaries/interfaces.[25,27,33,35]

From a mechanistic perspective, P3HT nanoaggregates formed upon ultrasonication grow into relatively longer fibrillar structures via anisotropic assembly of the nanoaggregates; upon UV irradiation, polymer chains present at the ends of the aggregates undergo a photoexcitation induced conformational change from "aromatic" (random coil conformation) to "quinoid" (linear or extended coil conformation),[25,36] The conformation change facilitates anisotropic assembly of the nanoaggregates in a direction perpendicular to the polymer backbone through $\pi-\pi$ interactions between the polymer chains existing at the ends of neighboring aggregates. Figure 2a presents a mechanistic illustration of the P3HT nanocrystallite assembly process. In a typical experiment, P3HT/$CHCl_3$ solution in a borosilicate glass vial is sealed with a cap, and then ultrasonicated in a table-top ultrasonic cleaner for relevant times as described in the literature, which results in the formation of highly crystalline P3HT nanoaggregates in the solution via a change in the polymer chain conformation (disorder−order transitions).[16] The highly ordered P3HT nanoaggregates appear short (less than 200 nm) in length owing to strong agitation associated with ultrasonication.[16,25] Subsequently, the ultrasonicated P3HT solution is stirred gently and exposed to UV irradiation for various times, leading to anisotropic assemblies of the crystalline nanoaggregates into longer fibrillar structures.

Figure 2b shows the clear evolution of a nanofibrillar morphology depending on ultrasonication and/or UV irradiation. Both P3HT1 and P3HT2 films appear featureless and amorphous-like in the absence of any irradiation of the corresponding solutions. This observation is ascribed to rapid solvent evaporation, which suppresses the formation of well-

Table 1. Molecular Weight and Regioregularity of the P3HT Samples Used

	molecular weight (kDa)		
P3HT sample	M_n	M_w	regioregularity (%)
P3HT1	19.7	43.7	96
P3HT2	34.6	69.0	92

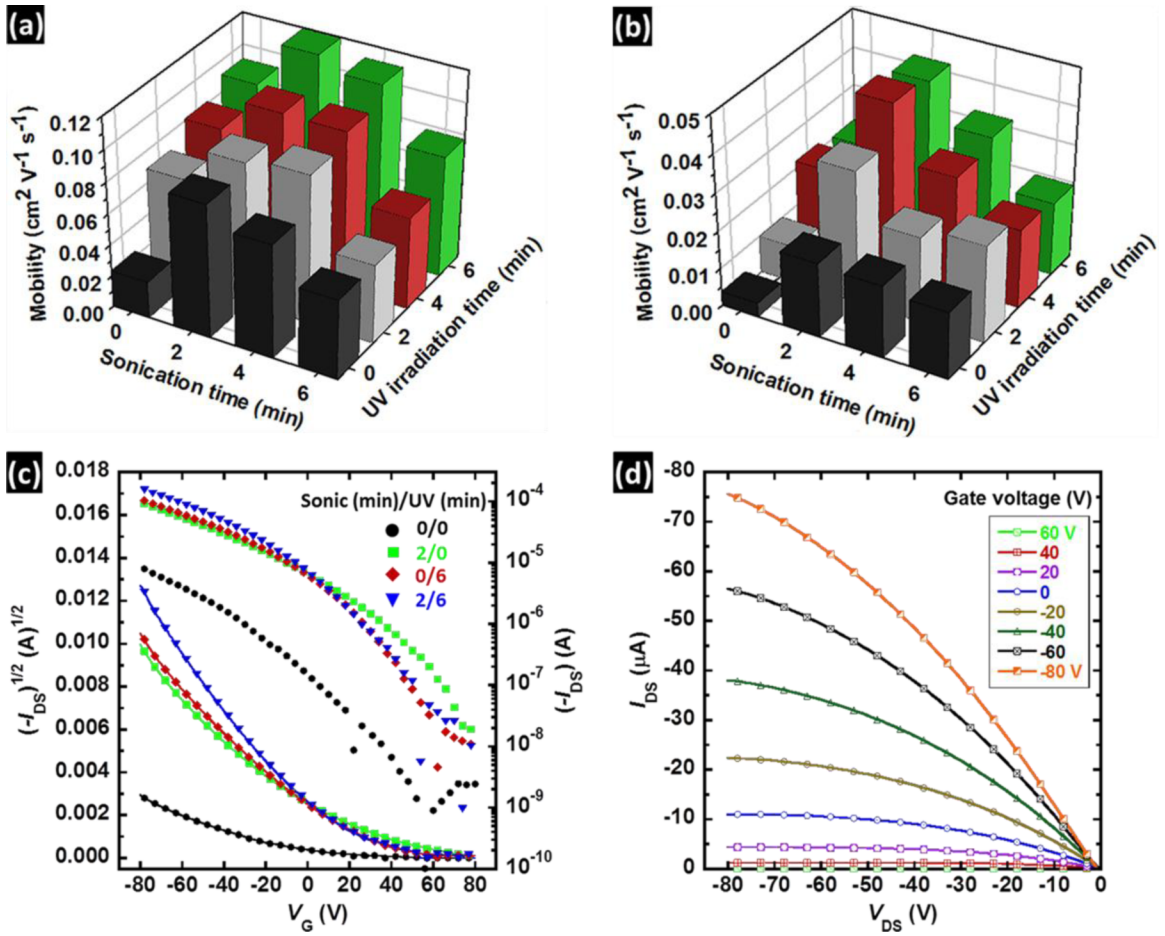

Figure 1. Average field-effect mobilities of (a) P3HT1 and (b) P3HT2 films spin coated from the polymer solutions treated to ultrasonication and/or UV irradiation for various times. Mobilities were calculated in the saturation regime of operation with $V_{DS} = -80$ V. (c) Transfer characteristics of P3HT1 OFET devices fabricated from pristine, 2 min ultrasonicated, 6 min UV irradiated, and sequential 2 min ultrasonicated and 6 min UV irradiated polymer solutions. (d) Typical output characteristics obtained from a P3HT1 OFET prepared via spin-coating from the polymer solution irradiated by sequential 2 min ultrasonication and 6 min UV irradiation. All measurements were performed in a nitrogen glovebox.

ordered structures.[15,16] Brief (2 min) ultrasonic irradiation of both solutions leads to the formation of short nanofiber-like structures (i.e., ∼30 nm in width and 120 nm in length for P3HT1 and ∼15 nm in width and 70 nm in length for P3HT2). It is generally accepted that both higher RR and MW leads to aggregates having wider fibrillar structures owing to a more planarized main chain conformation and longer weight-average contour length, respectively.[20,32] Consistent with previous reports,[20] RR is a more prominent factor than MW regards to P3HT nanoaggregation; the higher RR but lower MW P3HT1 forms wider aggregates, compared to P3HT2. Moreover, the higher RR materials exhibits longer fibrillar structures, which is attributed to more planarized polymer backbones facilitating favorable $\pi-\pi$ interactions between polymer chains.[25,37,38]

In contrast to ultrasonic irradiation, UV irradiation (6 min) tends to promote growth of fibrillar features into relatively longer units, however, there appear to be fewer such structures within resultant films.[25] After 2 min sonication and subsequent 6 min UV irradiation, surprisingly, the short nanofibrillar features obtained upon ultrasonication become longer (∼300 nm for P3HT1 and ∼150 nm for P3HT2), which supports the proposed mechanistic interpretation (Figure 2a). Examination of Figure 2c, which depicts the evolution of P3HT thin-film morphology for samples prepared from solutions sequentially treated with 6 min ultrasonication followed by 6 min UV irradiation provides additional evidence that sonication induced aggregates self-assemble into larger structures. As indicated by the green circle, smaller aggregates formed during ultrasonication for 6 min clearly assemble into longer, anisotropic fibrillar structures via subsequent UV treatment (6 min). Nanofiber length increased upon subsequent UV irradiation, suggesting a reduction in the number of grain boundaries between the initially formed nanofiber aggregates. The surface roughness of resultant films also changed upon ultrasonication and/or UV exposure. The pristine films were relatively smooth with a low root-mean square (RMS), ∼0.43 nm for P3HT1 and ∼0.39 nm for P3HT2, while that for films obtained from solutions that were sequentially subject to 2 min ultrasonication followed by 6 min UV irradiation gradually increasee to ∼1.89 nm and ∼0.82 nm for P3HT1 and P3HT2, respectively. The increased roughness is ascribed to the formation of nanofibrillar structures within the thin-films.

UV−visible spectral features strongly correlate with the extent of molecular ordering (intra- and intermolecular ordering) in π-conjugated polymer solutions and solid, thin-films.[25,39] Pristine P3HT solutions exhibit only high energy features ($\pi-\pi^*$ intraband transition) at ∼453 nm and ∼450 nm for P3HT1 and P3HT2, respectively. Upon ultrasonication and/or UV irradiation, low energy features appear at ∼567 and

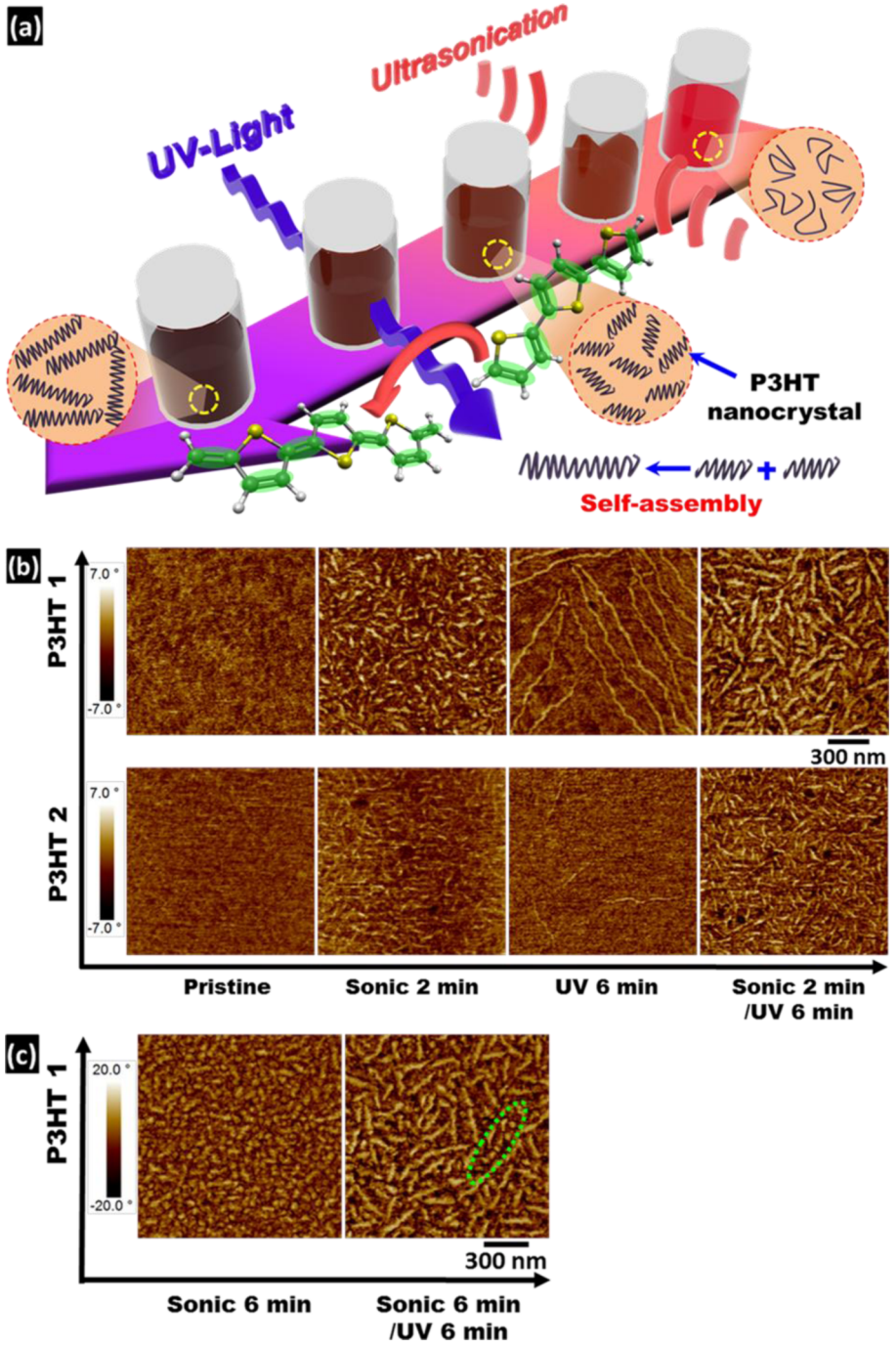

Figure 2. (a) Suggested mechanism describing the anisotropic assembly of P3HT nanocrystallites formed by ultrasonication into longer nanofibrillar structures via subsequent UV irradiation of the solution. (b) Tapping mode AFM phase images of P3HT1 and P3HT2 films obtained by spin-coating from the polymer solutions which were treated by ultrasonication and subsequent UV irradiation for 0 and 0 min, 2 and 0 min, 0 and 6 min, and 2 and 6 min, respectively. (c) Tapping mode AFM phase images of P3HT1 films spin-coated from 6 min ultrasonicated, and sequentially 6 min ultrasonicated and 6 min UV irradiated polymer solutions, respectively. The green circle surrounds a small P3HT nanocrystallite undergoing assembly into a fibrillar structure upon subsequent UV irradiation.

623 nm for P3HT1 and at ~558 and 617 nm for P3HT2, suggestive of vibronic bands associated with the (0−1) and (0−0) transitions, respectively[25,39] (Figure 3a and c). The emergence of these features is associated with interchain coupling.[40] For higher RR polymer (P3HT1), the lower energy features remarkably increase in the order UV irradiation (6 min) < ultrasonication (2 min) < sequential ultrasonication (2 min) and UV irradiation (6 min), supporting the premise that polymer chain intermolecular interactions increase in the solution state as a function of the given process. For the less RR material (P3HT2), the lower energy features also increase, but the effect is far less dramatic because of fewer $\pi-\pi$ stacking interactions arising from higher steric distortions of polymer chain backbone.

The UV−vis absorption trends observed in the CP solutions is carried through to the corresponding films; the solution based crystalline nanoaggregates survive the spin-coating process, and in turn provide for increased molecular ordering

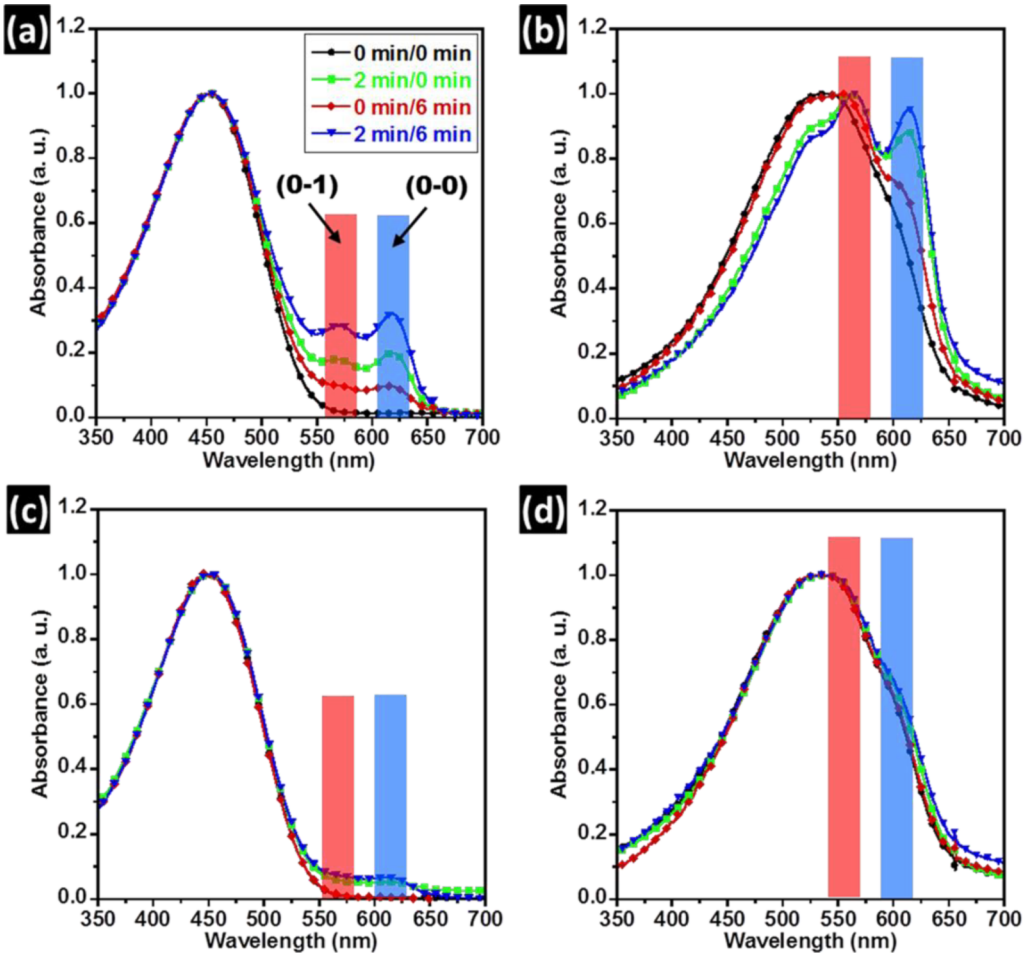

Figure 3. Normalized UV−visible absorption spectra of (a) P3HT1/$CHCl_3$ solutions under ultrasonication followed by UV irradiation for 0 and 0 min, 2 and 0 min, 0 and 6 min, and 2 and 6 min, respectively; and (b) corresponding P3HT1 films obtained by spin-coating. Normalized UV−visible absorption spectra of (c) P3HT2/$CHCl_3$ solutions treated by ultrasonication and subsequent UV irradiation for 0 and 0 min, 2 and 0 min, 0 and 6 min, and 2 and 6 min, respectively; and (d) corresponding P3HT2 films obtained by spin-coating.

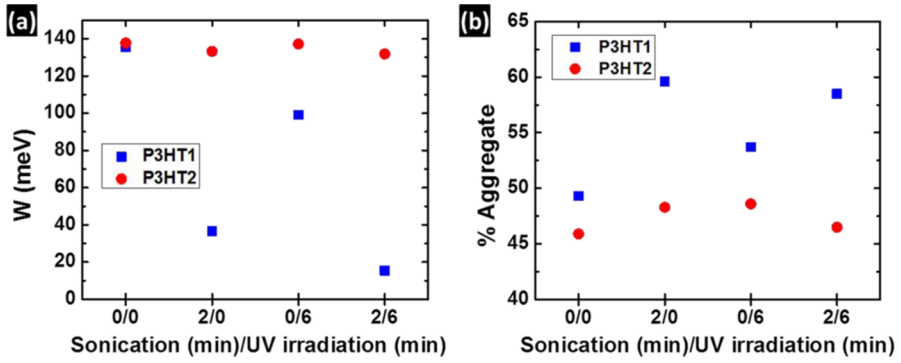

Figure 4. Evolution of (a) exciton bandwidth *W* and (b) percentage of ordered aggregates in the P3HT1 and P3HT2 films spin-coated from pristine, 2 min ultrasonicated, 6 min UV irradiated, and sequentially 2 min ultrasonicated and 6 min UV irradiated polymer solutions.

in the solid thin-films as shown in Figures 3b and d. Compared to pristine films, the lower energy features are red-shifted in films obtained from solutions subject to sequential 2 min sonication and 6 min UV irradiation (i.e., from ∼554 to 566 nm (0−1) and from ∼602 to 615 nm (0−0) for P3HT1 and from ∼547 to 550 nm (0−1) and from ∼598 to 604 nm (0−0) for P3HT2), owing to more planarized polymer chain backbones compared to those from pristine films.[16,25] In addition, the intensity of the (0−0) transition increases, relative to the (0−1) transition. The intensity differences indicate that sequential sonication and UV irradiation of the polymer solutions leads to enhanced intramolecular ordering within polymer chains in corresponding solidified films.[25,39,40]

Quantitative analysis of intra- and intermolecular ordering of polymer chains can be performed by means of static absorption spectroscopy and quantitative modeling.[39,40] The P3HT absorption spectrum is composed of two phases, a crystalline region due to ordered chains and an amorphous region due to

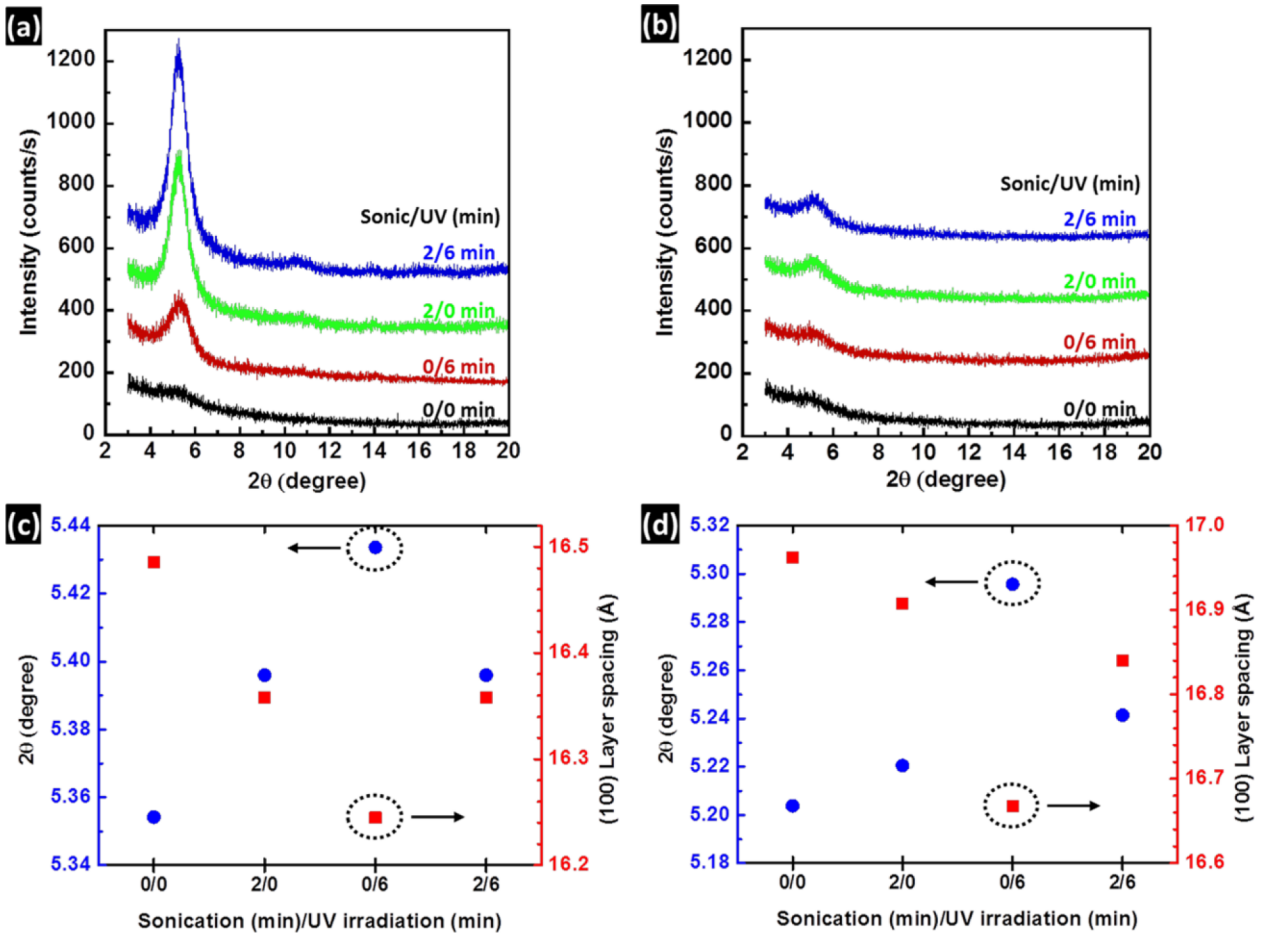

Figure 5. Grazing incidence X-ray diffraction profiles of (a) P3HT1 and (b) P3HT2 films obtained from pristine, 2 min ultrasonicated, 6 min UV irradiated, and sequentially 2 min ultrasonicated and 6 min UV irradiated polymer solutions. 2θ angle (left axis) of the (100) peak and corresponding layer spacing (right axis) of corresponding (c) P3HT1 and (d) P3HT2 films.

disordered chains.[40] According to Spano's model, interchain coupling leads to vibronic bands in the absorption spectrum.[40] Further, the vibronic bands can be related to the free exciton bandwidth (W), which correlates with intrachain ordering of an individual polymer chain within the aggregates.[25,39,40] An increase in intramolecular order leads to a decrease in W.[25,39,40] Equation 1 is used to calculate the W values, using the intensities of the (0−0) and (0−1) transitions obtained from fits to the experimental spectra (see Figures S2 and S3 in the Supporting Information).

$$\frac{I_{0-0}}{I_{0-1}} \approx \left(\frac{1 - 0.24W/E_p}{1 + 0.073W/E_p}\right)^2 \quad (1)$$

I_{0-0} and I_{0-1} represent the intensities of the (0−0) and (0−1) transitions, respectively and E_P is the vibrational energy of the symmetric vinyl stretch (taken as 0.18 eV).[40] As shown in Figure 4a, while W of P3HT1 films obtained from pristine solution appears at 135.6 meV, the value significantly decreases to 99.1, 36.6, and 15.4 meV after 6 min UV irradiation, 2 min ultrasonication, and sequential ultrasonication (2 min) followed by 6 min UV irradiation, indicative of enhanced intramolecular ordering of P3HT chains. In contrast, the W value decreases only slightly from 137.8 to 137.2, 133.3, and 131.9 meV for P3HT2 films obtained through the same treatments to the precursor solutions (Figure 4a).

The number of aggregates in the resultant films was also affected by ultrasonication and/or UV irradiation of the precursor solutions. The absorption contributions of the photophysical aggregates and amorphous P3HT regions can be separated using eq 2, which accounts for the effect of aggregates on the relative vibronic intensities, based on weakly interacting H-aggregates in polythiophenes.[39,40]

$$A \propto \sum_{m=0}\left(\frac{e^{-S}S^m}{m!}\right)\left(1 - \frac{We^{-S}}{2E_p}G_m\right)^2 \exp\left(-\frac{(E - E_{0-0} - mE_p - 1/2WS^m e^{-S})^2}{2\sigma^2}\right) \quad (2)$$

where A is the absorbance as a function of the photon energy (E), S is the Huang−Rhys factor (taken as 1.0),[40] G_m is a constant that depends on the vibrational level, m (for example, $m = 0$ for the (0−0) transition) as given by the equation, $G_m = \sum_{n(\neq m)} S^n/n!(n - m)$, where n is the vibrational quantum number, E_{0-0} is the 0−0 transition energy, and σ is the Gaussian line width. As shown in Figure 4b, the extent of aggregation was found to be ∼49.3% for pristine P3HT1 thin-films, and significantly increased to 53.7, 59.6, and 58.5%, respectively for films obtained from 6 min UV irradiated, 2 min ultrasonicated, and sequential 2 min ultrasonicated and 6 min UV irradiated solutions, suggesting increased P3HT chain intermolecular ordering. In contrast, the number of aggregates

from P3HT2 films also increased, but to a lesser extent, changing from ~45.9 to 48.6, 48.3, and 46.5%, which supports experimental results showing that lower RR P3HT is less sensitive to ultrasonication and/or UV irradiation induced changes associated with intermolecular ordering (Figure 4b).

The increased sensitivity to changes in intra- and intermolecular ordering of the higher RR P3HT polymer chains upon ultrasonication and/or UV irradiation, can also be understood in light of solubility effects. The more planar and rigid chain conformation associated with the higher RR material, afforded by fewer steric distortions imposed by the hexyl side chains, is expected to lead to lower solubility in solvents.[25,27] Thus, polymer−polymer interactions become more favorable than polymer−solvent interactions. Consistently, the aforementioned treatments to the higher RR P3HT dissolved in chlorobenzene and trichlorobenzene, both of which have better solubility relative to P3HT than $CHCl_3$, did not afford the spectroscopic changes observed for either $CHCl_3$ or toluene solutions (data not included).

The enhanced intra- and intermolecular interactions of P3HT chains are expected to lead to higher thin-film crystallinity.[15,25] Panels a and b in Figure 5 depict X-ray diffractograms obtained from grazing incidence (GIXD) measurements of P3HT1 and P3HT2 films spin-coated from the polymer solutions irradiated by sonication and/or UV for different times. The crystallinity of resultant films increases in order of UV irradiation (6 min), ultrasonication (2 min), and sequential ultrasonication (2 min) and UV irradiation (6 min), which is consistent with observed UV−visible spectral changes. Clearly, the XRD profiles reflect the enhanced polymer chain intra- and intermolecular ordering. The sequential treatment of P3HT precursor solutions to 2 min sonication and 6 min UV irradiation affords the highest intensity enhancement of the (100) peak, which is associated with polymer chain lamellar packing along the crystallographic direction perpendicular to the backbone.[16,25] This increase could be attributed to either an increase in the size of individual crystallites, the number of crystallites, or both.[16,25] In addition, the (100) peak of P3HT1 shifts to higher angle, from 5.35 to 5.40° (from a *d*-spacing of 16.49 to 16.36 Å) (Figure 5a), while the P3HT2 (100) peak shifts from 5.20 to 5.24° (from 16.96 to 16.84 Å) after the same treatment (Figure 5b), which suggests either increased interdigitation between P3HT alkyl side chains or a change in side chain tilt.[15,24]

CONCLUSIONS

In conclusion, this work demonstrates that sequential ultrasonication and UV irradiation of P3HT precursor solutions is an effective strategy to achieve a remarkable increase in mobility of corresponding films, without additional process steps such as dielectric surface modification and/or thermal or solvent vapor annealing. Small P3HT nanocrystallites formed via ultrasonication were anisotropically self-assembled into longer nanofibrillar structures by subsequent UV irradiation of the sonicated solutions. Consequently, enhanced intra- and intermolecular ordering with a concomitant reduction in grain boundaries within P3HT films was achieved via sequential ultrasonication and UV irradiation of the precursor solution, and contributes to the devices exhibiting excellent charge carrier transport properties ($\mu \approx 12.0 \times 10^{-2}$ cm^2 V^{-1} s^{-1} for 96% RR P3HT). The hole mobility of the lower RR P3HT also underwent a significant enhancement. Higher RR P3HT appears more sensitive to ultrasonication and/or UV irradiation induced changes in intra- and intermolecular ordering and the polymer chain nano- and microstructure. The approach described here is expected to be applicable to alternative π-conjugated polymer semiconductors and suitable for the fabrication of high-performance, large-area, flexible electronic devices for a wide range of commercial applications.

MATERIALS AND METHODS

Materials. P3HT1 was purchased from Rieke Metals Inc. and P3HT2 was purchased from Sigma-Aldrich Chemical Co., and were used without further purification. The molecular weight and regioregularity of both samples are summarized in Table 1. The molecular weight (MW) was obtained through gel permeation chromatography (GPC) using trichlorobenzene as the eluent and polystyrene as the standard. The head to tail regioregularity (RR) was estimated from the 1H-NMR spectra obtained from deuterated chloroform solution at 293 K using a Bruker DSX 300. Chloroform used in this study was anhydrous grade, purchased from Sigma-Aldrich, and used without further purification.

Anisotropic Growth of Conjugated Polymer Aggregates in the Solution. Ten mg of polymer was introduced into 2 mL of chloroform in a 20 mL borosilicate glass vial in air. Subsequently, the vial was sealed with a cap and the solution was stirred for at least 30 min at approximately 55 °C to completely dissolve the polymer. The as-prepared solution was cooled to ambient temperature, and in turn the solution was treated by ultrasonication and/or UV irradiation for relevant times:

(1) The ultrasonic irradiation of P3HT solutions was performed by following the same procedure as outlined in the literature.[16] A table top ultrasonic cleaner (Bransonic 2510, 40 kHz, ~0.4 W cm^{-2}) was used for ultrasonication of the solution. The sealed glass vials were immersed in the water bath of the ultrasonic cleaner, and then irradiated for relevant times (from 0 to 6 min).

(2) To conduct UV irradiation of the solution, we placed the vial containing the solution on a hand-held UV lamp (Entela UVGL-15, 5 mW cm^{-2}, 254 nm) which had been placed on a magnetic stirrer (Corning inc.). Then, the solution was gently stirred and irradiated using the lamp for times ranging from 0 to 6 min. The irradiation was performed through the bottom wall of the borosilicate glass vial, which transmits more than 90% of the incident 254 nm light.

(3) For sequentially combined ultrasonication and UV irradiation experiments, ultrasonic irradiation was performed first on the sealed glass vial for times ranging from 0 to 6 min, and then subsequently exposed to UV irradiation for times also ranging from 0 to 6 min.

Organic Field-Effect Transistor (OFET) Fabrication and Characterization. The OFET devices used for electrical characterization consisted of two contact devices where P3HT films were deposited via spin-coating the relevant polymer solution onto a 300 nm thick SiO_2 gate dielectric. The highly doped substrate wafer served as the gate electrode while Au/Cr was used for the source and drain contacts. The source and drain contacts were fabricated using a standard photolithography based lift-off process, followed by E-beam evaporation (Denton Explorer) of 50 nm Au contacts with 3 nm of Cr as the adhesion layer. Before spin-coating P3HT solutions, all devices were cleaned for 15 min in a UV-ozone cleaner (Novascan PSD-UV) to completely remove any residual photoresist and other organic contaminants. OFET devices were prepared by spin-coating (WS-650MZ-23NPP, Laurell) the solutions onto precleaned substrates at a spin speed of 1500 rpm for 60 s in air, and tested in nitrogen ambient using an Agilent 4155C semiconductor parameter analyzer. The P3HT1 and P3HT2 films obtained by spin-coating were found to have a thickness in the range of 36−48 nm and 33−38 nm, respectively as determined by spectroscopic ellipsometry (M-2000, JA Woollam). The devices were stored in a vacuum oven (1 Torr) overnight at room temperature to remove residual solvent. The field-effect mobility was

calculated in the saturation regime of transistor operation (V_{DS} = −80 V) by plotting the drain current (I_{DS}) versus gate voltage (V_{GS}) and fitting the data to the following equation

$$I_{DS} = \frac{WC_{OX}}{2L}\mu(V_{GS} - V_T)^2 \quad (3)$$

where W (2000 μm) and L (50 μm) are the transistor channel width and length, respectively, V is the threshold voltage, and C_{OX} is the capacitance per unit area of the silicon dioxide gate dielectric (1.15×10^{-8} F/cm^2).

UV−Vis Spectroscopy. The solution and solid state UV−vis spectra were recorded using an Agilent 8510 UV−vis spectrometer. Films for solid state studies were prepared by spin-coating the requisite solution onto precleaned glass slides following the same procedures used to prepare OFET devices.

Grazing Incidence X-ray Diffraction (GIXD). Out-of-plane grazing incidence X-ray diffraction data were obtained using a PanalyticalX'Pert Pro system equipped with a Cu X-ray source operating at 45 kV and 40 mA. The grazing incidence angle was fixed at 0.2° and the detector was scanned from 3 to 30°.

Atomic Force Microscopy (AFM). The AFM measurements were performed on films spin-coated onto bottom contact OFET devices using an ICON dimension scanning probe microscope (Bruker) operating in tapping mode with a silicon tip (RTESP, Bruker).

■ ASSOCIATED CONTENT

Ⓢ Supporting Information

Table of average field effect mobilities, thickness for the films spin-coated from the solutions sonicated for various times, and the results of fits to UV−vis absorption spectra. This material is available free of charge via the Internet at http://pubs.acs.org.

■ AUTHOR INFORMATION

Corresponding Author

*E-mail: ereichmanis@chbe.gatech.edu.

Funding

The authors declare no competing financial interest.

Notes

The authors declare no competing financial interest.

■ ACKNOWLEDGMENTS

The financial support of the Georgia Institute of Technology and the Air Force Office of Scientific Research (FA9550-12-1-0248) is gratefully acknowledged.

■ REFERENCES

(1) Burroughes, J. H.; Bradley, D. D. C.; Brown, A. R.; Marks, R. N.; Mackay, K.; Friend, R. H.; Burns, P. L.; Holmes, A. B. Light-Emitting-Diodes Based on Conjugated Polymers. *Nature* **1990**, *347*, 539−541.

(2) Friend, R. H.; Gymer, R. W.; Holmes, A. B.; Burroughes, J. H.; Marks, R. N.; Taliani, C.; Bradley, D. D. C.; Dos Santos, D. A.; Bredas, J. L.; Logdlund, M.; Salaneck, W. R. Electroluminescence in Conjugated Polymers. *Nature* **1999**, *397*, 121−128.

(3) Han, T. H.; Lee, Y.; Choi, M. R.; Woo, S. H.; Bae, S. H.; Hong, B. H.; Ahn, J. H.; Lee, T. W. Extremely Efficient Flexible Organic Light-Emitting Diodes with Modified Graphene Anode. *Nat. Photonics* **2012**, *6*, 105−110.

(4) Thomas, S. W.; Joly, G. D.; Swager, T. M. Chemical Sensors Based on Amplifying Fluorescent Conjugated Polymers. *Chem. Rev.* **2007**, *107*, 1339−1386.

(5) Huang, H. M.; Wang, K.; Tan, W. H.; An, D.; Yang, X. H.; Huang, S. S.; Zhai, Q.; Zhou, L.; Jin, Y. Design of A Modular-Based Fluorescent Conjugated Polymer for Selective Sensing. *Angew. Chem., Int. Ed.* **2004**, *43*, 5635−5638.

(6) Janata, J.; Josowicz, M. Conducting Polymers in Electronic Chemical Sensors. *Nat. Mater.* **2003**, *2*, 19−24.

(7) You, C. C.; Miranda, O. R.; Gider, B.; Ghosh, P. S.; Kim, I. B.; Erdogan, B.; Krovi, S. A.; Bunz, U. H. F.; Rotello, V. M. Detection and Identification of Proteins Using Nanoparticle-Fluorescent Polymer 'Chemical Nose' Sensors. *Nat. Nanotechnol.* **2007**, *2*, 318−323.

(8) Park, S. H.; Roy, A.; Beaupre, S.; Cho, S.; Coates, N.; Moon, J. S.; Moses, D.; Leclerc, M.; Lee, K.; Heeger, A. J. Bulk Heterojunction Solar Cells with Internal Quantum Efficiency Approaching 100%. *Nat. Photonics* **2009**, *3*, 297−302.

(9) Li, G.; Zhu, R.; Yang, Y. Polymer Solar Cells. *Nat. Photonics* **2012**, *6*, 153−161.

(10) Lipomi, D. J.; Tee, B. C. K.; Vosgueritchian, M.; Bao, Z. N. Stretchable Organic Solar Cells. *Adv. Mater.* **2011**, *23*, 1771−1775.

(11) Kim, B. G.; Jeong, E. J.; Chung, J. W.; Seo, S.; Koo, B.; Kim, J. S. A Molecular Design Principle of Lyotropic Liquid-Crystalline Conjugated Polymers with Directed Alignment Capability for Plastic Electronics. *Nat. Mater.* **2013**, *12*, 659−664.

(12) Qiu, L. Z.; Lee, W. H.; Wang, X. H.; Kim, J. S.; Lim, J. A.; Kwak, D.; Lee, S.; Cho, K. Organic Thin-Film Transistors Based on Polythiophene Nanowires Embedded in Insulating Polymer. *Adv. Mater.* **2009**, *21*, 1349−1353.

(13) Sirringhaus, H. Device Physics of Solution-Processed Organic Field-Effect Transistors. *Adv. Mater.* **2005**, *17*, 2411−2425.

(14) Ikawa, M.; Yamada, T.; Matsui, H.; Minemawari, H.; Tsutsumi, J.; Horii, Y.; Chikamatsu, M.; Azumi, R.; Kumai, R.; Hasegawa, T. Simple Push Coating of Polymer Thin-Film Transistors. *Nat. Commun.* **2012**, *3*, 1176.

(15) Chang, M.; Choi, D.; Fu, B.; Reichmanis, E. Solvent Based Hydrogen Bonding: Impact on Poly(3-hexylthiophene) Nanoscale Morphology and Charge Transport Characteristics. *ACS Nano* **2013**, 5402−5413.

(16) Aiyar, A. R.; Hong, J. I.; Nambiar, R.; Collard, D. M.; Reichmanis, E. Tunable Crystallinity in Regioregular Poly(3-hexylthiophene) Thin Films and Its Impact on Field Effect Mobility. *Adv. Funct. Mater.* **2011**, *21*, 2652−2659.

(17) Hamilton, R.; Smith, J.; Ogier, S.; Heeney, M.; Anthony, J. E.; McCulloch, I.; Veres, J.; Bradley, D. D. C.; Anthopoulos, T. D. High-Performance Polymer-Small Molecule Blend Organic Transistors. *Adv. Mater.* **2009**, *21*, 1166−1171.

(18) Allard, S.; Forster, M.; Souharce, B.; Thiem, H.; Scherf, U. Organic Semiconductors for Solution-Processable Field-Effect Transistors (OFETs). *Angew. Chem., Int. Ed.* **2008**, *47*, 4070−4098.

(19) Goffri, S.; Muller, C.; Stingelin-Stutzmann, N.; Breiby, D. W.; Radano, C. P.; Andreasen, J. W.; Thompson, R.; Janssen, R. A. J.; Nielsen, M. M.; Smith, P.; Sirringhaus, H. Multicomponent Semiconducting Polymer Systems with Low Crystallization-Induced Percolation Threshold. *Nat. Mater.* **2006**, *5*, 950−956.

(20) Aiyar, A. R.; Hong, J. I.; Reichmanis, E. Regioregularity and Intrachain Ordering: Impact on the Nanostructure and Charge Transport in Two-Dimensional Assemblies of Poly(3-hexylthiophene). *Chem. Mater.* **2012**, *24*, 2845−2853.

(21) Liu, J.; Arif, M.; Zou, J.; Khondaker, S. I.; Zhai, L. Controlling Poly(3-hexylthiophene) Crystal Dimension: Nanowhiskers and Nanoribbons. *Macromolecules.* **2009**, *42*, 9390−9393.

(22) Oh, J. Y.; Shin, M.; Lee, T. I.; Jang, W. S.; Min, Y.; Myoung, J. M.; Baik, H. K.; Jeong, U. Self-Seeded Growth of Poly(3-hexylthiophene) (P3HT) Nanofibrils by a Cycle of Cooling and Heating in Solutions. *Macromolecules* **2012**, *45*, 7504−7513.

(23) Sirringhaus, H.; Brown, P. J.; Friend, R. H.; Nielsen, M. M.; Bechgaard, K.; Langeveld-Voss, B. M. W.; Spiering, A. J. H.; Janssen, R. A. J.; Meijer, E. W.; Herwig, P.; de Leeuw, D. M. Two-Dimensional Charge Transport in Self-Organized, High-Mobility Conjugated Polymers. *Nature* **1999**, *401*, 685−688.

(24) Park, Y. D.; Lee, H. S.; Choi, Y. J.; Kwak, D.; Cho, J. H.; Lee, S.; Cho, K. Solubility-Induced Ordered Polythiophene Precursors for High-Performance Organic Thin-Film Transistors. *Adv. Funct. Mater.* **2009**, *19*, 1200−1206.

(25) Chang, M.; Lee, J.; Kleinhenz, N.; Fu, B.; Reichmanis, E. Photoinduced Anisotropic Supramolecular Assembly and Enhanced

Charge Transport of Poly(3-hexylthiophene) Thin Films. *Adv. Funct. Mater.* **2014**, *24*, 4457−4465.
(26) Kim, D. H.; Jang, Y.; Park, Y. D.; Cho, K. Surface-Induced Conformational Changes in Poly(3-hexylthiophene) Monolayer Films. *Langmuir* **2005**, *21*, 3203−3206.
(27) Aiyar, A. R.; Hong, J. I.; Izumi, J.; Choi, D.; Kleinhenz, N.; Reichmanis, E. Ultrasound-Induced Ordering in Poly(3-hexylthiophene): Role of Molecular and Process Parameters on Morphology and Charge Transport. *ACS Appl. Mater. Interfaces* **2013**, *5*, 2368−2377.
(28) Chang, J. F.; Sun, B. Q.; Breiby, D. W.; Nielsen, M. M.; Solling, T. I.; Giles, M.; McCulloch, I.; Sirringhaus, H. Enhanced Mobility of Poly(3-hexylthiophene) Transistors by Spin-Coating from High-Boiling-Point Solvents. *Chem. Mater.* **2004**, *16*, 4772−4776.
(29) Fu, Y.; Lin, C.; Tsai, F. Y. High Field-Effect Mobility from Poly(3-hexylthiophene) Thin-Film Transistors by Solvent-Vapor-Induced Reflow. *Org. Electron.* **2009**, *10*, 883−888.
(30) Cho, S.; Lee, K.; Yuen, J.; Wang, G. M.; Moses, D.; Heeger, A. J.; Surin, M.; Lazzaroni, R. Thermal Annealing-Induced Enhancement of the Field-Effect Mobility of Regioregular Poly(3-hexylthiophene) Films. *J. Appl. Phys.* **2006**, *100*, 114503.
(31) Kline, R. J.; McGehee, M. D.; Kadnikova, E. N.; Liu, J. S.; Frechet, J. M. J. Controlling the Field-Effect Mobility of Regioregular Polythiophene by Changing the Molecular Weight. *Adv. Mater.* **2003**, *15*, 1519−1522.
(32) Zhang, R.; Li, B.; Iovu, M. C.; Jeffries-EL, M.; Sauve, G.; Cooper, J.; Jia, S. J.; Tristram-Nagle, S.; Smilgies, D. M.; Lambeth, D. N.; McCullough, R. D.; Kowalewski, T. Nanostructure Dependence of Field-Effect Mobility in Regioregular Poly(3-hexylthiophene) Thin Film Field Effect Transistors. *J. Am. Chem. Soc.* **2006**, *128*, 3480−3481.
(33) Chua, L. L.; Zaumseil, J.; Chang, J. F.; Ou, E. C. W.; Ho, P. K. H.; Sirringhaus, H.; Friend, R. H. General Observation of n-type Field-Effect Behaviour in Organic Semiconductors. *Nature* **2005**, *434*, 194−199.
(34) Crossland, E. J. W.; Tremel, K.; Fischer, F.; Rahimi, K.; Reiter, G.; Steiner, U.; Ludwigs, S. Anisotropic Charge Transport in Spherulitic Poly(3-hexylthiophene) Films. *Adv. Mater.* **2012**, *24*, 839−844.
(35) Wu, P. T.; Xin, H.; Kim, F. S.; Ren, G. Q.; Jenekhe, S. A. Regioregular Poly(3-pentylthiophene): Synthesis, Self-Assembly of Nanowires, High-Mobility Field-Effect Transistors, and Efficient Photovoltaic Cells. *Macromolecules* **2009**, *42*, 8817−8826.
(36) Kim, Y. H.; Spiegel, D.; Hotta, S.; Heeger, A. J. Photoexcitation and Doping Studies of Poly(3-hexylthienylene). *Phys. Rev. B: Condens. Matter. Phys.* **1988**, *38*, 5490−5495.
(37) Cheng, Y. J.; Yang, S. H.; Hsu, C. S. Synthesis of Conjugated Polymers for Organic Solar Cell Applications. *Chem. Rev.* **2009**, *109*, 5868−5923.
(38) Son, H. J.; Carsten, B.; Jung, I. H.; Yu, L. P. Overcoming Efficiency Challenges in Organic Solar Cells: Rational Development of Conjugated Polymers. *Energy Environ. Sci.* **2012**, *5*, 8158−8170.
(39) Zhao, K.; Khan, H. U.; Li, R. P.; Su, Y. S.; Amassian, A. Entanglement of Conjugated Polymer Chains Influences Molecular Self-Assembly and Carrier Transport. *Adv. Funct. Mater.* **2013**, *23*, 6024−6035.
(40) Clark, J.; Chang, J. F.; Spano, F. C.; Friend, R. H.; Silva, C. Determining Exciton Bandwidth and Film Microstructure in Polythiophene Films Using Linear Absorption Spectroscopy. *Appl. Phys. Lett.* **2009**, *94*, 163306.